University of Exeter coursework header sheet

ECM3101 Individual Project (Beng) (A, TRM1+2 2017/8)

077965

1032716

650026037

Coursework: Final Report

Submission Deadline: Wed 9th May 2018 12:00

Personal tutor: Professor Yanqiu Zhu

Marker name: N/A

Word count: 9801

By submitting coursework you declare that you understand and consent to the University policies regarding plagiarism and mitigation (these can be seen online at www.exeter.ac.uk/plagiarism, and www.exeter.ac.uk/mitigation respectively), and that you have read your school's rules for submission of written coursework, for example rules on maximum and minimum number of words. Indicative/first marks are provisional only.

First marker's comments

Indicative mark

Second marker's comments

Second mark

Moderator's comments

Agreed mark

Final Report

Modelling the Flow of Excess Powder in Additive Layer Manufacturing

Edward Hayes

2018

3rd Year Individual Project

I certify that all material in this thesis that is not my own work has been identified and that no material has been included for which a degree has previously been conferred on me.

Signed: Edward Hayes.

College of Engineering, Mathematics, and Physical Sciences
University of Exeter

Final Report

ECM3101

Title: Modelling the Flow of Excess Powder in Additive Layer Manufacturing

Date of submission: Wednesday, 9th May 2018

Student Name: Edward Hayes
Programme: Mechanical Engineering BEng
Student number: 650026037
Candidate number: 077965

Supervisor: Professor Gavin Tabor

Abstract

The following report is an investigation into modelling the flow of excess powder from additive layer manufacturing. In recent years, additive layer manufacturing has grown rapidly. A major drawback with ALM is the post-processing stage, if this was made more efficient, ALM could move from small-scale uses such as rapid prototyping, to manufacturing on a larger scale. Finite element analysis will be used to calculate the frequency that the parts resonate at making the maximum displacement of the oscillations, leading to more efficient powder flow. The discrete element method (DEM), will be used to provide a numerical model for the flow of excess powder. As this is a relatively recent application for DEM, a process has been developed in this report to effectively build up a model of the removal of excess powder using the specific modal vibrations for the individual components. Starting with a relatively small number of particles to provide a basic model of powder flow and then working up to around 50,000 particles to work towards a much more accurate and realistic model. This led to a successful model of the flow of excess powder from the components tested.

Keywords: Powder, Discrete Element Modelling, Additive Layer Manufacturing

Table of contents

Table of Figures

Table of Tables

1. Introduction and background

This following report is an investigation into the removal of excess powder from additive layer manufacturing (ALM). This involves the use of the Discrete Element Method, (DEM), to determine how the powder behaves when particles come into contact with each other. Finite Element Analysis, (FEA), will also be used to work out how different components behave while vibrating. These two methods will be coupled together to build a successful model of the removal of powder from the post-processing stage of ALM.

1.1. Outline of the problem

Additive Layer Manufacturing is a relatively recent class of manufacturing method whereby components are made via the building up of two-dimensional layers. [1]This allows for a greater degree of complexity to geometry that can be made compared to traditional manufacturing techniques such as casting and moulding. It is also less wasteful and energy intensive than subtractive manufacturing techniques such as CNC milling. In recent years, ALM has grown rapidly from uses outside of rapid prototyping and it is seen by many as a future rival for traditional manufacturing techniques.

[2]This project will focus on powder based ALM methods such as Selective Laser Sintering (SLS) and Selective Laser Melting (SLM). Liquid resin, as well as solid filaments, are used in other techniques which require a different post-processing method. SLS and SLM both operate in a very similar way. This process starts by laying a bed of powder on a movable platform, which is subsequently heated to just below its melting point. A laser is then used to scan the two-dimensional cross-section of the component being made. The laser causes the powder to be fused together. The platform is then moved downward at a distance equal to the thickness of each layer, and a new layer of powder is laid down. This process is then repeated building up the part layer upon layer until the part is complete.

Where the two processes differ is that SLS uses the unmelted bed of powder to support subsequent layers that might overhang and be unsupported. [1] SLS parts tend to be less dense and porous compared to SLM which have a higher density and are stronger. This is because SLM re-melts the previous layer so that the individual layers join. For this reason, SLM components are heavier and therefore sometimes require a support structure.

Once the process is complete, the finished component needs to be removed from the powder bed. Excess powder on the outside of the part can easily be removed; this is usually achieved by brushing the additional powder away. For hollow components such as tubes, the internal powder is much more difficult to remove; this is normally done via vibration.

In this investigation, the vibration of components will be modelled using Finite Element Analysis, and the behaviour of the powder will be modelled using Discrete Element Method. The results from these will then be brought together and conclusions drawn to successfully produce a model for the removal of excess powder from ALM.

1.2. Finite Elements

[3]Finite Element Analysis, FEA, is used by engineers to simulate the behaviour of solid physical bodies. It computationally solves multiple differential equations that would not be possible to do by hand. FEA is used to improve designs and observe where there are weaknesses in a structure. [4] The effect of stress on the object can clearly be shown; using this knowledge, adjustments can be made prior to manufacture. This leads to a reduced number of prototypes that need to be made. In this investigation, the Finite Element Analysis will be carried out on ANSYS.

1.3. Discrete Element Method

[5]The Discrete Element Method is a computational model that predicts the behaviour of granular materials and geomaterials. The technique is used for various applications from large bulk solids such as rocks and soils to fine particles like powders and pellets. DEM is a computationally heavy model, as each individual interaction between the particles is calculated.

The software that will be used in this project is EDEM, which is the market leading software for DEM simulations, meaning that there are a lot of resources and tutorials that can be followed.

2. Literature review

In recent years, there have been many research studies concerning additive layer manufacturing. Currently, there are no published works on using DEM to model the flow of excess powder from ALM, but there have been numerous studies investigating DEM for ALM as well as using DEM for applications further afield including in geotechnics and the pharmaceutical industry. Reading a broad selection of projects from different areas has led to a greater understanding of the subject and the discrete element method as a whole.

2.1. Literature from ALM

[6]O Skrinjar provided an overview of how discrete element modelling is currently being used to model powder in ALM. The report mainly focused on compaction in the bed of powder and how the powder packs together. This introduced how DEM could be applied to an ALM process. Another investigation by C.L. Martin, [7] gave further inside to this application discussing the effect of sintering of the particles effect of the density. These two investigations were incredibly useful for providing an overview of how DEM could be used to model an ALM process but did not add additional information about the effect of vibrations and the post-processing requirements.

2.2. Literature from Other Areas

The experimental procedure was difficult to obtain and develop from looking solely at sources concerning ALM, because of this it was necessary to investigate other disciplines to give a greater understanding of using DEM with vibrations. W R. Ketterhagen [8] produced a study that investigated how DEM could be used to model particles in the pharmaceuticals industry. The study gave insight into contact models as well as the effect of particle size which will be discussed further in section 3.2.2. The importance of model validation was made clear but as there are far too many particles to be able to calculate a physical validation model must take place to validate results. This information was useful as it dealt with almost identical particle size, the majority of available literature mainly concerned for uses in geotechnics and mining applications. These studies became useful when developing an experimental procedure. H Lee, [9]provided how vibrations can be coupled with DEM. The study aimed to predict the breakages of particles in a centrifugal/vibration mill. Although it was dealing with larger bulk materials and at lower oscillatory values, the information obtained was useful in giving insight into reducing the time simulations took to run.

3. Methodology and theory

3.1. Modal Analysis

3.1.1. Theory

Modal analysis studies the vibration in solid bodies, which have very few inputs but a high number of outputs. A modal analysis will be used to find out the natural frequencies of the different parts that have designed for further use during this investigation. [10]The natural frequency can be defined as:

> The rate at which an object vibrates when it is not disturbed by an outside force.

The different degrees of freedom each have their own natural frequency. These frequencies relate to the speed of the vibration travelling through the object as well as the wavelength. Most bodies can be forced into resonance; this is the point where small forces lead to large oscillatory deflections in the solid body.

[11]The modes of a solid body are determined by several factors such as mass, initial boundary conditions and the stiffness of the material. The stiffness of the material is highly significant as it acts as the restoring force acting against the deflection which causes oscillations. It is difficult to find individual vibration mode shapes, as many modes tend to be excited at similar frequencies, so it is difficult to distinguish between them.

Due to the complexity and having a high amount of outputs, as well as being difficult to distinguish different mode shapes, Finite Element Analysis (FEA) is used to solve these problems computationally. [12] Modal analysis is one of the most common forms of FEA alongside linear static analysis. It is the simplest form of FEA as it does not deal with loading

and other external forces as it is calculated from the shape of the geometry, due to the resonate frequencies only being related to the constraints on the model as well as its shape.

The mode shapes will be relevant to this project as it will show how different parts vibrate differently. The frequencies, as well as the direction of the deformation, will be used to model the vibrations of the part in the DEM section of this report.

3.1.2 Methodology

The modal analysis was carried out using ANSYS Workbench. The following is the method and procedure that was followed [13].

1. The initial stage is to input the geometry; this can be done by importing a CAD file or by sketching it in the Design Modeler. For this project, the CAD files were imported from Solidworks; it was essential to make them one continuous part, instead of separate extrude joined together. This is because the parts will be made by ALM instead of being welded together. It is vital to ensure that designs have fully defined geometry and are converted to an STL file.
2. Once the geometry is imported, the mesh can be generated. A mesh divides up the given geometry into a smaller and more manageable domain to allow for computational simulation. The small sections of the overall geometry are known as elements, which are used to solve equations. The smaller the elements become, the closer the computational model will represent an actual model; the smaller elements become, the longer the computational simulation will take. It is good to start with a larger mesh size to start with relatively few elements to ensure that the analysis can simulate quickly, the mesh can be adjusted afterwards to ensure accuracy in the results.
3. Before running the simulation, the number of modes needed to be found must be inputted. The first six modes found are rigid body modes rather than vibration modes. Rigid body modes are not considered in this investigation, and thus, will be ignored. For all geometries, the first three vibration modes were found.
4. The time it takes for the simulation to run will be determined by the number of elements. Once the simulation is finished, the mode shapes will need to be evaluated, which will allow for animations of the vibration modes to be produced. From this information, the direction of the deformation can be inferred.
5. A mesh convergence study will need to take place to improve the accuracy of the results. [14]Mesh convergence is a process of refining the mesh using ever smaller elements to work towards a more accurate result. In this instance, this was achieved by plotting the value of the first modal frequency against the number of elements used in the mesh. This process is called a mesh convergence curve. As the number of plot points increases, the curve will start to asymptote towards the true value. Once the gradient of the curve tends towards zero - where large changes in the number of elements lead to very small successive changes in the first modal frequency - the model can be classed as converged.

6. The mesh can be refined so that it is finer at areas of interest and larger elements are used in regions of less importance. [15]This process is known as local mesh refinement. In this project, local mesh refinement was not used as all the parts were relatively geometrically consistent and straightforward; therefore, it was not necessary.

3.2. Discrete Element Method

3.2.1. Properties of ALM Powder

[16] [17]The properties of a component made by SLM are greatly dependent on the properties of the powder used. The morphology of the powder, which is its initial shape and size, can have drastic consequences on the components density and strength. The quality of the final component is also affected by things such as the surface roughness. There are three main ways of producing metallic powders for ALM. [18] The first is via mechanical milling; this is where powders are manufactured from larger pieces of materials and cut down and shaped into small powder. The second is plasma atomization; a plasma torch is used to melt a metal wire causing molten metal to fall creating spherical particles. The final is the most common form; gas atomization. [19] This is where molten metal is forced via a stream of inert gas, such as nitrogen, through a nozzle; when it cools, it forms metallic spheres. Both plasma atomisation and gas atomisation form very spherical and regular particles. Whereas, mechanical milling forms irregularly shaped powders. Spherical powders are desirable as they can pack closer together increasing the density of the final component. They behave more predictably and consistently, leading to a higher quality product. Irregular powders tend to produce more porous components as they cannot pack together as tightly, which leads to gaps in the structure. In certain instances, these properties can be desirable.

The size of the particles, as well as the regularity of the particle size, has drastic effects on the powders flowability. [17]The typical range for the diameter of the powder is between 10 µm and 45 µm Very fine particles, less than 5 µm, tend to cluster together. On the other hand, larger particles which are greater than 90 µm, reduce the packing density. In some instances, a combination of fine and larger particles is used so that the finer powders fill the voids left in the gaps between larger powder particles, which leads to a very high density.

3.2.2. Contact Models

In EDEM many different particle contact models can be used, these simulate how bulk materials behave when individual particles come into contact with one another. When different solids collide a combination of forces and moments are produced which makes modelling the collision of particles difficult. [20]The discrete element method has different approaches when considering modelling the collision between particles.

- The first is a hard sphere approach; this does not model the deformation of particles when they collide with each other meaning there is no deformation at the contact area. This model relies on an assumption of minimal contact time and the velocity of the

particles after the collision are calculated from the equations of motion and coefficient of restitution.

- The second method is a soft sphere approach; this does take into consideration the deformation of particles. This is done by looking at how much particles would overlap when they collide which can be used to calculate a deformed contact area.

The hard sphere approach can be simulated much quicker than the more complex soft sphere approach. There are eight contact models pre-programmed into EDEM each of which has its own set of laws and equations which models the interaction between these particles.

1. Hertz-Mindlin (no slip) [21]
   The default, and most commonly used interaction model is the Hertz-Mindlin. This is used to model the behaviour of dry as well as elastic bulk solids which accounts for the majority of DEM use such as mixing powders in the pharmaceutical industry. This is an example of an elastic model with non-adhesive contact, meaning that energy losses between the particles are not considered as well as the different contact bodies being separate as adhesive forces are not present. The model makes a few assumptions; such as there is no friction between the continuous contact area. In addition to this, it is assumed that the strains are within the elastic limit of the material. It uses the integration of Hooke's law over the area of deformation which results in the model being non-linear.

2. Hertz-Mindlin (no slip) with RVD Rolling Friction [22]
   This combines all the complexities and accuracies of the Hertz-Mindlin model in addition to including rolling friction. The rolling friction is the force that acts against the motion of a rolling body; in this context, it is applied by the particles rolling on the boundary layer as well as on each other. It is calculated from the known coefficient of rolling resistance and the relative velocity of the particle including the deformations at the contact area. This function is most commonly used for larger bulk solids, such as rocks instead of small particles such as powders.

3. Hertz-Mindlin with JKR [22]
   To add the complexity of adhesion forces, Johnson, Kendall and Roberts came together to formulate a model that included the coming together of particles and the effect of contact pressure. This was done by combining the stored elastic energy of the particle while subtracting the loss in surface energy.

4. Hertz-Mindlin with bonding [22]
   This model takes into consideration intermolecular forces into account when the particles collide. This allows for the calculation of a resultant force caused by the overlap of the particles, which is calculated from the total force in the tangential and normal directions.

5. Hertz-Mindlin with heat conduction [23]
   The last of the Hertz-Mindlin contact models that include how the particles respond under different temperatures and how thermal conductivity is affected by the size of the particle.

6. Linear Cohesion [24]
   Used for finding solutions for the combination of cohesive granular solids normally in the form of particles being compressed together to form a new particle. An example of this would be in the pharmaceutical industry where the powder is compressed in a mould to form a tablet.

7. Linear Spring [25]
   This is an example of a linear contact model that uses the soft sphere approach to model the contact of particles. It relies on the principles of Hooke's law, where the overlap between the particles is used to calculate their deformation which is then multiplied by the spring stiffness constant of the material.

8. Hysteric Spring [26]
   A simple, non-linear contact model. It is very similar to the Linear Spring contact model. A key difference is that a different spring constant is used for the deformation of the particle upon contact to the spring constant restoring the particle to its equilibrium shape.

This project will use the standard Hertz-Mindlin contact model, as it is good for dealing with fine dry powders. It will model the contact between particles well enough but without hindering the speed of the simulation.

3.2.3. Methodology

[27]EDEM is made up of three distinct sections;

- EDEM creator, which allows you to set up bulk materials equipment and contact models.
- EDEM simulator, which runs the simulation to model how the bulk solids behave.
- EDEM analyst, which is used to show the simulation in a visual form as well as obtain data and graphs.

The following is the method used in the EDEM creator to run a simulation:

1. The bulk material, which is the material of the particle needs to be defined. [28]This can be done by going into the library of known materials or manually entering the properties of the desired materteral. The key material property is the shear modulus which is a measure of stiffness parallel to the surface of the material. Typical values range between $1x10^6$ and $1x10^9$. These relate to the shear modulus of the individual particles that make up the powder, and not the powder as a collective. Values used are

typically lower than actual values as the particles are small, and thus, they behave differently due to a variety of reasons, such as the lack of dislocations. A lower value is also used, due to the higher the shear modulus used, the longer the simulation takes to run. The interactions between the different particles need to be inputted. These include:

- Coefficient of Restitution, [29] is the ratio of velocities before and after a collision between two colliding objects. This ranges from 0, for inelastic collisions to 1, for perfectly elastic collision. Typical values for bulk solids are around 0.5.
- Coefficient of Static Friction, [30]describes the ratio between the frictional force between the two particles. The typical value for bulk solids is around 0.5.
- Coefficient of Rolling Friction, [31] this is similar to the coefficient of static friction but is for the particles rolling against each other. The typical value for bulk solid will range between 0 and 0.2.

2. Once the properties of the bulk material are defined, the size and shape of the particles can be made. [32]The way particles are made is by building up different spheres, the distance between the particles as well as their radius can be used to create differently shaped particles. The smaller the radius of the sphere, the shorter the time step so the simulation will take more time to run. As particles, in reality, are not going to do be identical, a size distribution can be applied using the standard deviation meaning all the particles will be unique but within a given range. The mass of the particle can be calculated by inputting the desired values, or EDEM can calculate it automatically. A CAD file of a particle can be imported to aid aesthetics of the simulation. The geometry of the CAD file is not used in the calculations but must be modelled using a combination of spheres to define the shape.

3. The equipment material, which makes up the physical boundaries of the simulation, needs to be entered in a similar way to the bulk material. [28]Unlike before, the values for the shear modulus do not affect the time the simulation takes to run. The interaction between the bulk solid and material also needs to be inputted with typical values similar to before.

4. Geometries can be added either by creating shapes in the EDEM creator or by importing a CAD file. [33]Creating geometry is done by making shapes either from, cuboids, cylinders or polygons; these can be merged to make different equipment. [34]CAD can be imported by either IGES, STEP or STL files. The shape of the geometry does not affect the time step, so even if the geometry is more complicated, the simulation will not take more time to run. The size of the geometry does affect the time step, the larger the geometry in relation to the size of the particles. Geometries can either be physical, which means they will use the data inputted from the

equipment material or virtual where they do not act as a solid boundary and allow particles to pass through them without hindrance.

5. A factory is required to add particles to an EDEM simulation. A factory is a piece of geometry that defines a region within the EDEM simulator where particles are created. Factories can either be made from a closed physical part making a closed volume or from a virtual part. There are two types of factory:

    - A static factory; [35]creates all required particles in a single timestep. Once all the particles have been created, the factory is classed as complete, and the simulation moves onto the next time step. This is used to fill volumes quickly. A static factory can either entirely fill a volume, generate a discrete number of particles or generate a specific mass of particles.
    - A dynamic factory; [36] acts over multiple timesteps allowing the material to be generated continuously. A dynamic factory can either generate an unlimited number of particles, a discrete number of particles or a specific mass of particles. The rate of generation can also be controlled.

6. Kinematics can be added to the equipment; this can be done by adding rotations as well as translations. [37] Kinematics can either be linear, so they start at one place and end in another, sinusoidal, where they oscillate between two positions at a fixed frequency or conveyor, where the equipment is stationary, but the particles move relative to it modelling a conveyor belt.

7. The contact model needs to be selected to determine how the particles will interact with each other as well as with equipment. These are shown in section 3.2.2.

8. The environment section controls external forces applied to the particles and the size of the domain. [38] External forces such as gravity can be applied to any direction and can be turned off.

Once the simulation is set up in EDEM creator, it can be processed in the EDEM simulator. Euler is the default integration method. [39] A Rayleigh time step approach is used to ensure stability, this is the maximum ideal time step that could be used in a simulation. The value is calculated from the material properties such as the shear modulus and the minimum radius size. In the majority of cases, the calculated Rayleigh time step is too large; this would mean an increase in simulation time. Typically, 20% of the Rayleigh time steps to ensure stable simulations that do not take up too much time. The length of time of the simulation also needs to be set, the longer the time period, the longer the simulation will take to run.

The simulator grid is used in the EDEM algorithms to determine where particles collide. A grid cell size is recommended to be three times as large as the minimum radius of a particle. The smaller the grid size, the longer it takes simulations to run, as this investigation is about

modelling powder the grid size needs to be this small. For modelling larger particles such as rock such a small grid size is not necessary.

Once the simulation is complete, the results can be analysed in EDEM analyst, which allows play through individual time steps.

4. Experimental work

This section will explain the experimental procedure, as well as detailing how the project has developed and evolved throughout the process.

4.1. Creating Parts to be Tested

Four designs were produced in Solidworks to be tested. All these designs had the same internal and external radius meaning that the wall thickness was consistent across all models. The tubes were all made in the same way using the sweep tool; this would make sure that all tubes were continuous rather than connecting individual extrudes and cuts, as this more accurately reflects a single ALM part. All the tubes had the same length of 150 mm at the centre of the pipe to ensure consistency between the models.

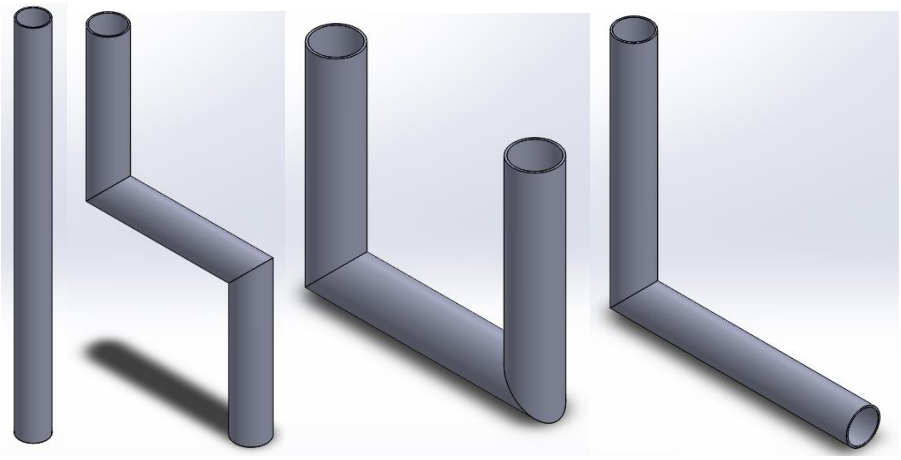

Figure 1 showing the different tubes that will be tested

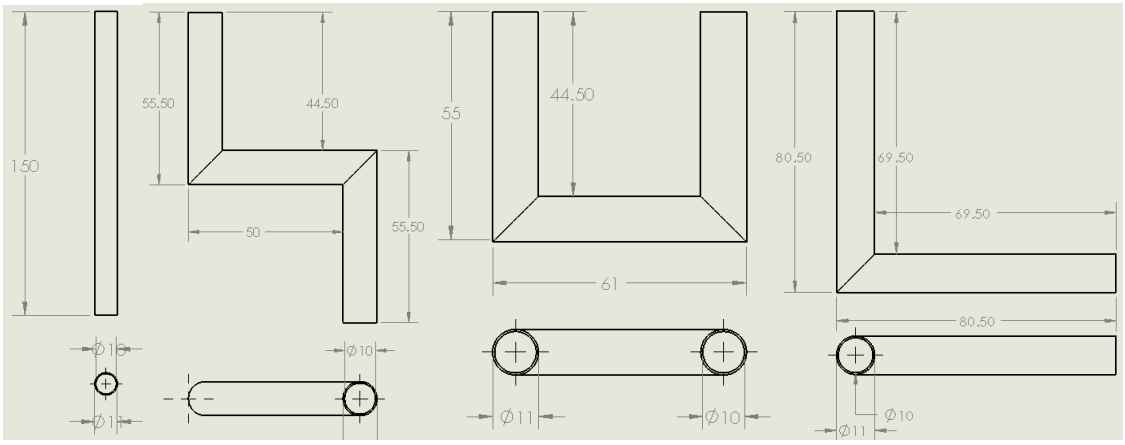

Figure 2 showing the dimensions of the different tubes with the dimensions shown in mm

The tubes, (see figures 1 and 2) will be referred to later as Straight tube, S tube, U tube and V tube labelled from left to right. The tube walls are constant and in each case are 0.5 mm thick and have an internal diameter of 10mm.

4.2. Modal Analysis

The experimental procedure for the Modal Analysis did not differ from the methodology. As stated in section 3.1.2, a mesh convergence study was used to ensure an appropriate number of elements were used. As the number of elements increased, the more the result tended to the actual value.

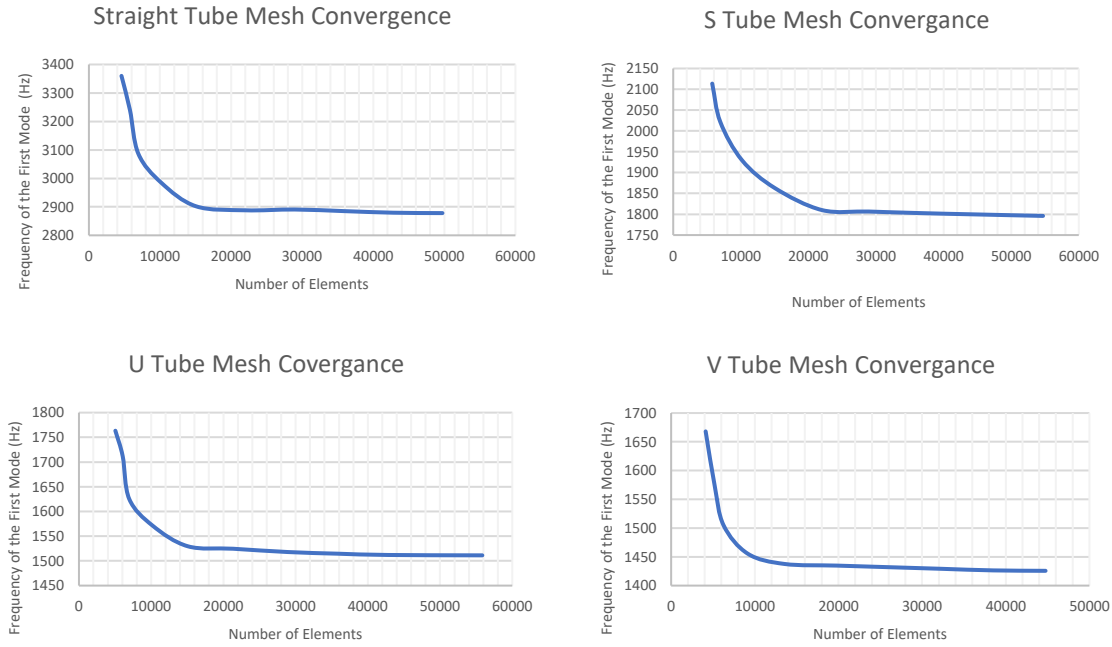

Figure 3 showing the mess convergence curves for each of the tubes

4.3. Discrete Element Method

EDEM requires a lot of computational resources and accurate, detailed solutions that take a long time to simulate. [8] [9]The smaller particles that are used, the longer the simulation takes to run, which is important in this case as the particles used are very fine. Similar to FEA - where a relatively small number of elements are used on initial experiments to check the accuracy of the model - this project developed a similar approach, whereby only a small number of particles, were simulated in the tubes. If a small number of particles did not escape from the tube at a specific modal frequency than it was almost certain that a larger sample of particles would not be able to escape. The mode shapes that successfully removed all the particles were taken forward to model a larger number of particles. This process improves efficiency by using a small number of particles that make simulations run quicker than if a large sample of particles were used. Thus, time would not be wasted accurately recording unsuccessful mode shapes.

4.3.1. Experimental Set Up

For conclusions to be drawn between the different simulations, they were all set up correspondingly. Each tube was tested for its first three modal frequencies, using the results from the modal analysis. The oscillations of the tubes were modelled by sinusoidal translations at a frequency equal to the modal shape. Although this was not an exact representation of the mode shape at that frequency, the displacement and direction of oscillation of the mode shape were used for the sinusoidal. This was as accurate as could be expected, considering the geometry in EDEM is rigid and cannot deform to match the modal shape.

The material that is going to be used in this investigation is an alloy of Titanium called Ti–6Al–4V, this is one of the most commonly used alloys of titanium. It has a very high strength to density ratio, and there is vast experience in manufacturing it. In ALM, it is commonly used to make implants and prosthetics which are customised to the individual's needs. In addition, it is commonly used in the aerospace industry. [40]Key properties such as a density of 4400 kg/m^3 were used as this did not affect the length of the time step as well as the Poisson's ratio of 0.342.

The shear modulus, which has a great effect on the time step was selected at $1x10^7$ Pa for the bulk solid and $1x10^8$ Pa for the equipment material. Although these are significantly smaller than the typical value for Ti–6Al–4V of 40 GPa, the bulk solid will have a much lower value for its shear modulus due to it being a powder and as the equipment has been made via ALM it will not have the same properties as if it was made via a traditional manufacturing technique. These smaller values were chosen as they will not increase the time step dramatically but are accurate enough to represent this titanium alloy.

Following the research before the investigation, the particles were made spherical as this is the shape of most powder particulates used in ALM as it allows for efficient packing. One of the largest approximations came from the size of the powder. The radius has the greatest effect on the time step; a radius of $1x10^{-4}$ m was used, the smaller radius was tried but either they did not work, or there was not enough computational memory. This radius leads to the particles being approximately twice-the-size of a coarse powder and 20 times the size of a fine powder. The particles have a fixed radius ensuring that all were identical, which speeds up their generation. Other calculated properties of the powder are shown in the table below:

Mass	$1.68x10^{-8}$ kg
Volume	$4.19x10^{-12}$ m^3
Moment of Inertia	$6.7x10^{-17}$ kgm^2

Table 1 showing details of the particle

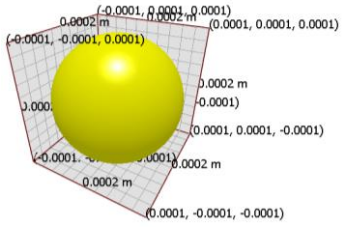

Figure 4 showing the dimensions of the particles used

In all models, except if otherwise stated, gravity will act downward in the z-direction. As discussed in section 3.2.2, the contact model applied will be the Hertz-Mindlin (no slip), as this is best for dealing with dry powders.

The table below shows the values that define the interactions between the particles as well as between the particles and the geometry.

Coefficient of Restitution	0.5
Coefficient of Static Friction	0.5
Coefficient of Rolling Friction	0.01

Table 2 defining the interactions between the particles

A standard value of 0.5 was used for the coefficients of restitution and static friction. A smaller value for the coefficient of rolling friction was used which can be expected for fine powders.

4.3.2. Dynamic Factory

The first successful results that were obtained came from using dynamic factories. A virtual polygon was used as the source of the particles, so it created them and allowed particles to pass through it unhindered. The experiment was set up as shown below in figure 5.

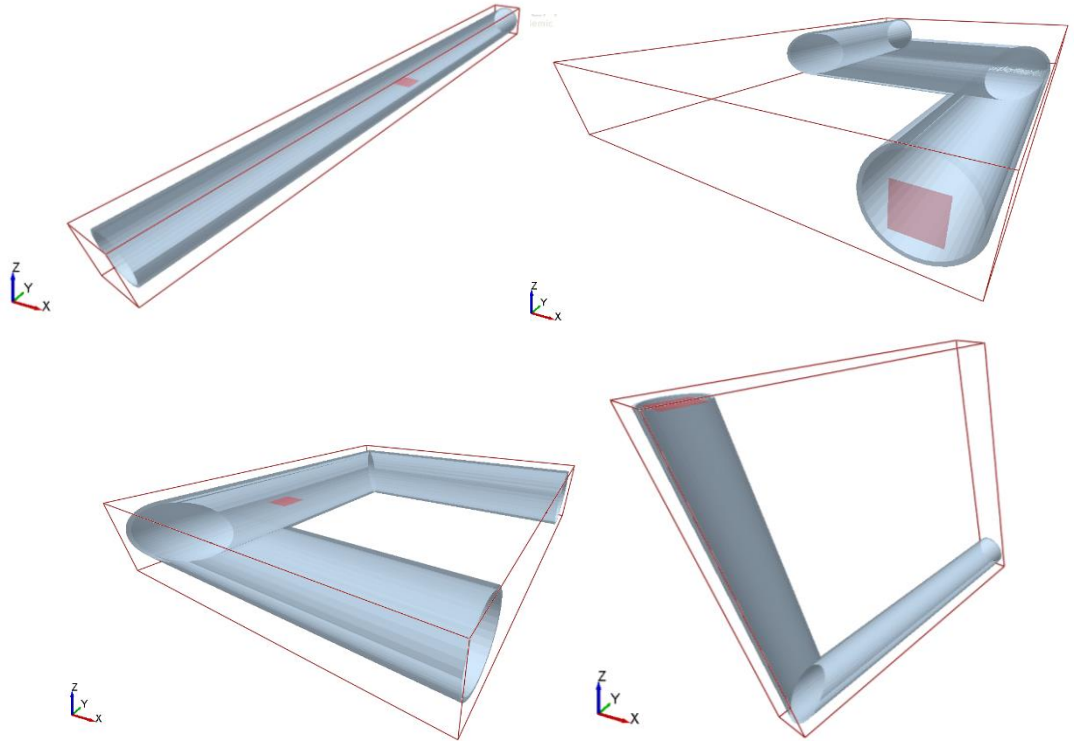

Figure 5 showing the setup of the dynamic factories

In all cases, the set up was the same except for the S tube, where gravity was acting in the y direction instead of the negative z direction. This allowed the particles to enter each tube and flow through, if the vibrations were to allow it. The factories created 500 particles at a generation rate of 5000 particles per second. Initially, simulations ran for 5 seconds but this was shortened as most relevant information was gained from the first couple of seconds. If particles could not pass through there would be little point in investigating a detailed solution, as this would take up too much time.

4.3.3. Static Factory

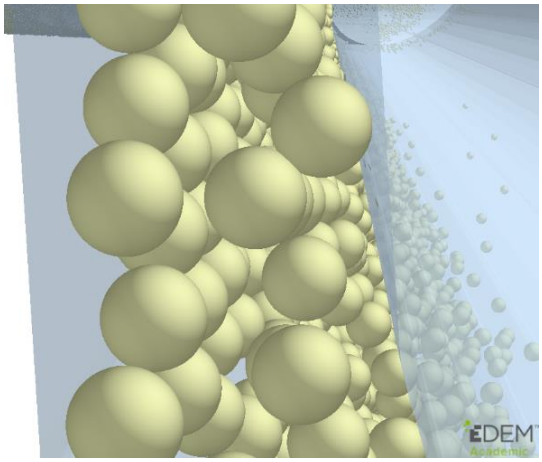

To build up a more realistic model more particles would need to be used, this was achieved by using a static factory. The purpose of this will be to fill the component with particles and then find how they are affected by the vibrations. A static factory can only be formed in a closed volume, in this instance particles were only generated between the two walls of the tubes. The hope of this was to find out how a larger number of particles interact with the boundary layer. This was a good way of focussing on how the particles interact at the boundary layer as this is the only place they are generated.

Figure 6 showing the generation of particles between the boundary layer

4.3.4. Internal Static Factory

A model was produced of having the tube full of particles at the beginning and then vibrating it, to tie together the results from the dynamic factory and the static factory, which builds up a picture of what happens to the particles in the tube and at the boundary layer retrospectively. This was achieved by making a CAD file that mapped out the internal walls of the tubes; this geometry could then be imported and placed inside the original geometry. Just as before, the original geometry would oscillate with a sinusoidal vibration. The internal geometry would not oscillate and would be made virtual so that it did not interfere with the particles. This allows for the tube to be filled after the initial timestep.

5. Presentation of experimental or analytical results/descriptions of final constructed product

5.1. Modal Analysis Results

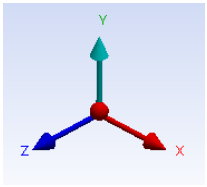

The following section contains the results of the modal analysis. All the tubes are orientated the same way per figure 7. The maximum deformation is shown in the red areas and the minimum in blue.

Figure 7

5.1.1. Straight Tube

The straight pipe is symmetrical in the x and z directions, as you would expect, this means that the first four modal frequencies are the same. For this reason, the first five mode shapes are calculated.

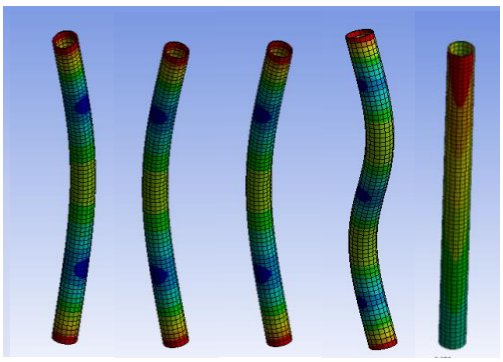

Mode	Frequency (Hz)	Deformation (mm)	Direction
1st	2878	14.2	X and z
2nd	7496	14	X and z
3rd	10434	10.72	y

Table 3 showing the modal frequencies of the straight tube

Figure 8 1st x, 1st z, 2nd x, 2nd z, 3rd y modes for the straight tube

5.1.2. S Tube

The S tube is not symmetrical although there is rotational symmetry, because of this the first three vibration modes are individual and distinct. All the modes happen at a similar frequency.

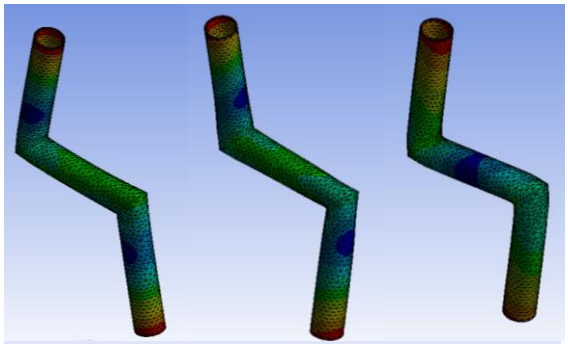

Mode	Frequency (Hz)	Deformation (mm)	Direction
1	2109.3	14.7	x
2	2130.1	15.7	z
3	2608.2	13.4	y

Table 4 showing the modal frequencies of the S tube

Figure 9 showing the 1st, 2nd and 3rd modal shapes

5.1.3. U Tube

The U tube had 3 very different mode shapes each in the x y and z direction at distinct frequencies.

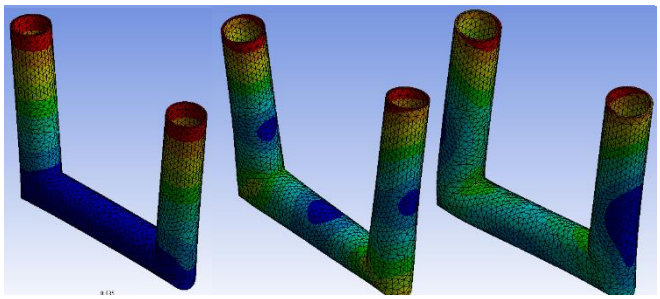

Mode	Frequency (Hz)	Deformation (mm)	Direction
1	1511.2	15.6	x
2	2390.4	15.6	z
3	2964.3	14	y

Table 5 showing the modal frequencies of the U tube

Figure 10 showing the 1st, 2nd and 3rd modal shapes

5.1.4. V tube

As the V tube is simply two straight tubes joined at a 90° angle, the results show the first two modes vibrating in the z direction as if they were straight tubes. The third mode has the two tubes vibrating in different directions, the tube parallel to the y axis is vibrating in the x direction and the tube parallel to the x axis is vibrating in the y direction.

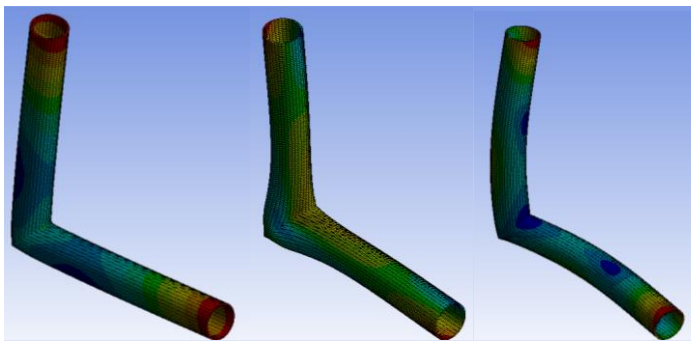

Mode	Frequency (Hz)	Deformation (mm)	Direction
1	1425.7	17.3	z
2	5030	16.4	z
3	6739	14.5	x and y

Table 6 showing the modal frequencies of the V tube

Figure 11showing the 1st, 2nd and 3rd modal shapes

5.2. *Example DEM results*

5.2.1. Dynamic Results

The purpose of these results is not to build an accurate model of the flow of excess powder but to see if the specific frequency was sufficient enough to remove all powder. The creation rates were different in each case; therefore, some of the graphs initially fluctuate, caused by several reasons such as the performance of the computer and the size of the factory. If the factory was too small, the flow rate of particles into the simulation was slowed down as the particles cannot be touching when they are created.

5.2.1.1. Straight Tube

It was decided that only the first vibration frequency would be tested in the x and z direction as by initial investigations the higher frequencies in the same direction behaved almost identically.

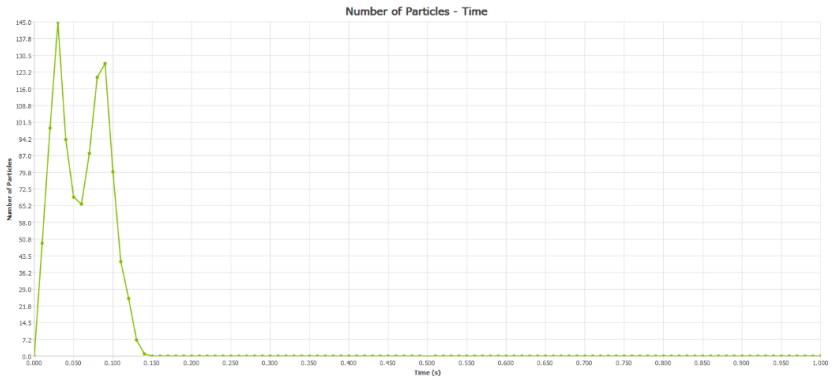

Figure 12 Straight Tube First Mode x direction

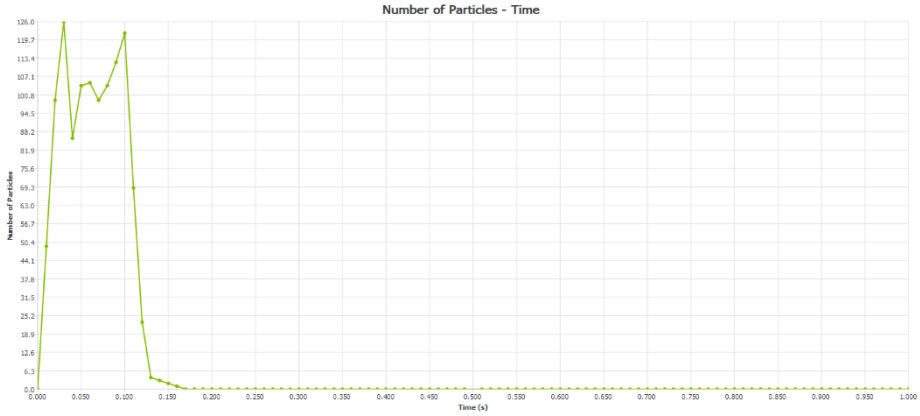

Figure 13 Straight Tube First mode z direction

The small number of particles easily passed through the system in both the x and z directions; therefore, both tubes will be taken to the nest stage for further investigation.

5.2.1.2. S Tube

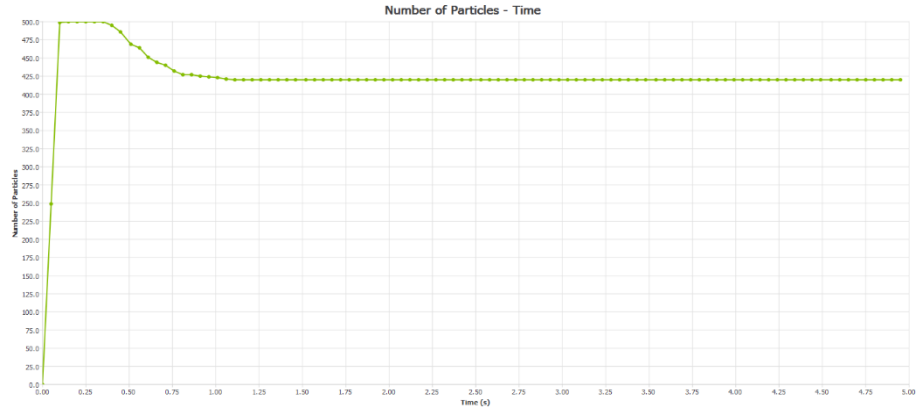

Figure 14 S Tube, First Modal Frequency

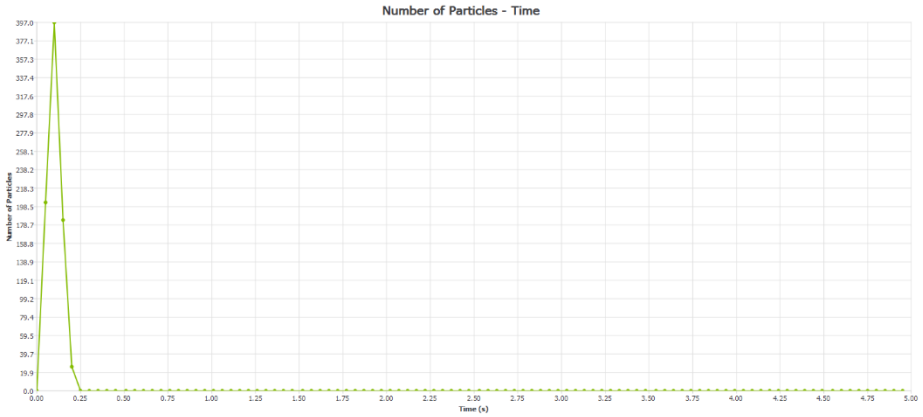

Figure 15 S Tube, Second Modal Frequency

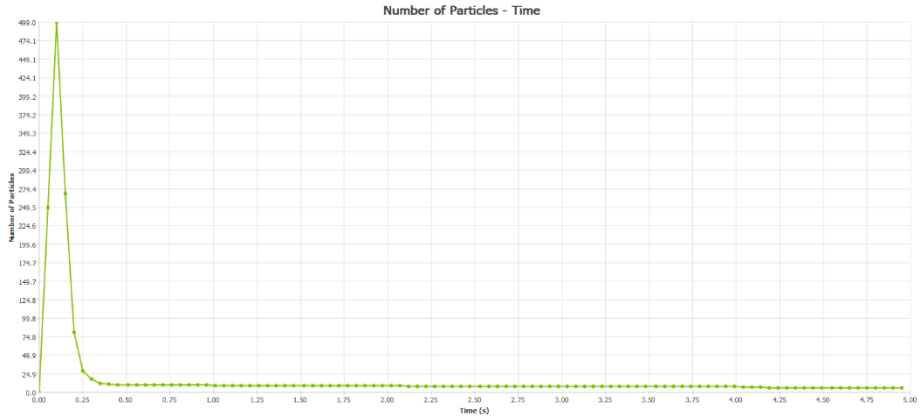

Figure 16 S Tube, Third Modal Frequency

Only the second modal frequency was able to transport all the particle through it. The initial few particles from the first modal frequency managed to escape, but then it quickly plateaued. Although the third modal frequency had a similar initial flow, a small number of particles were stuck oscillating at the first 90˚ bend. As shown below:

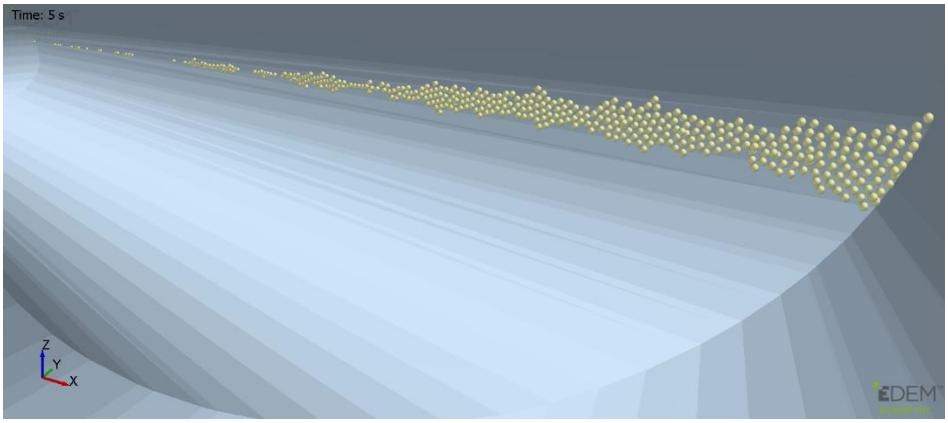

Figure 17 showing inside the s tube at 5 second for the first modal frequency

The direction of oscillation was not sufficient to remove the particles for the first and third modal frequencies, so they will be ignored for the next stage of the results.

5.2.1.3. U Tube

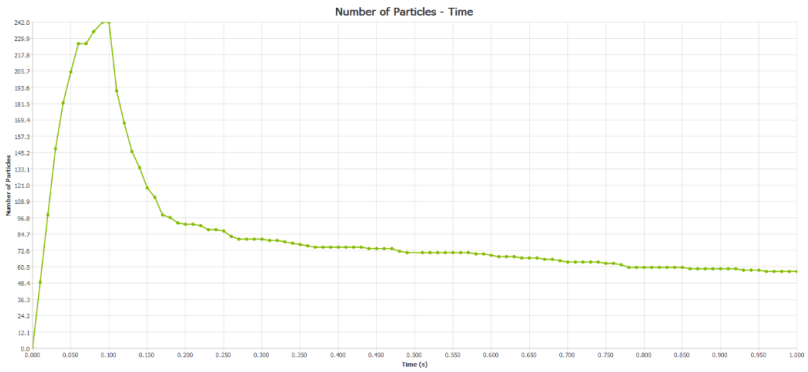

Figure 18 U Tube, First Modal Frequency

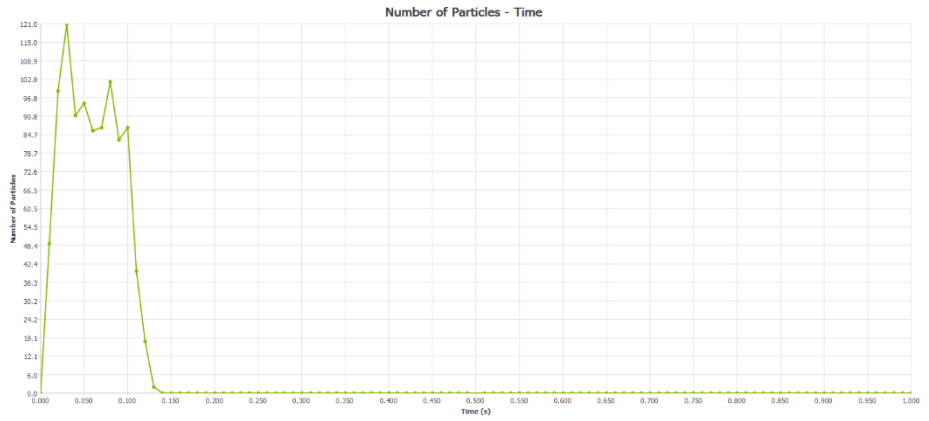

Figure 19 U Tube, Second Modal Frequency

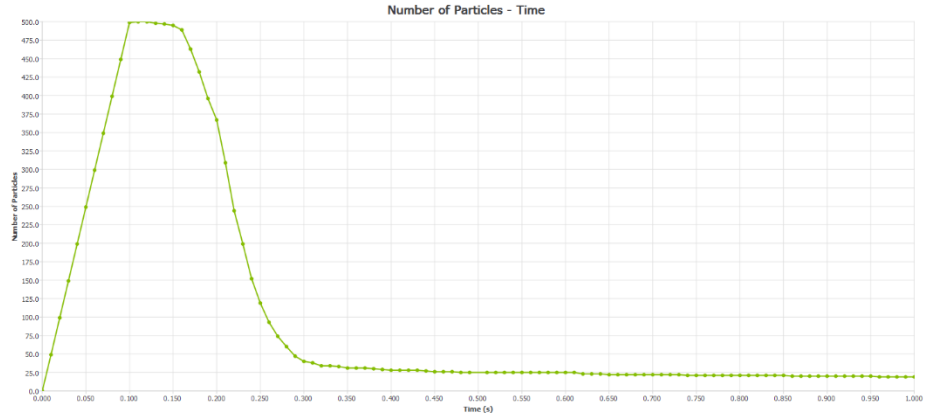

Figure 20 U Tube, Third Modal Frequency

The second mode was the only U tube that allowed all the particles to flow though it in the given time frame. The first and third mode are still decreasing but are decreasing at a much slower rate than initially. Further investigation would be required to see if all particles will leave the system. To maximise efficiency of the time to run simulation in this report only the second mode will be taken to the next stage of the investigation.

5.2.1.4. V Tube

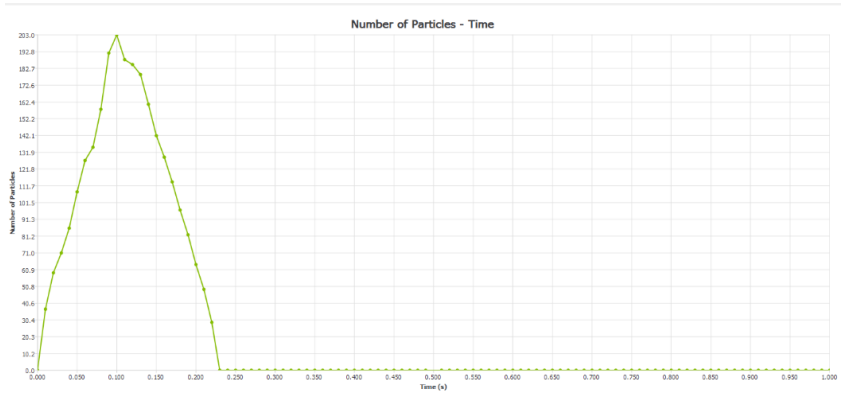

Figure 21 V Tube, First Modal Frequency

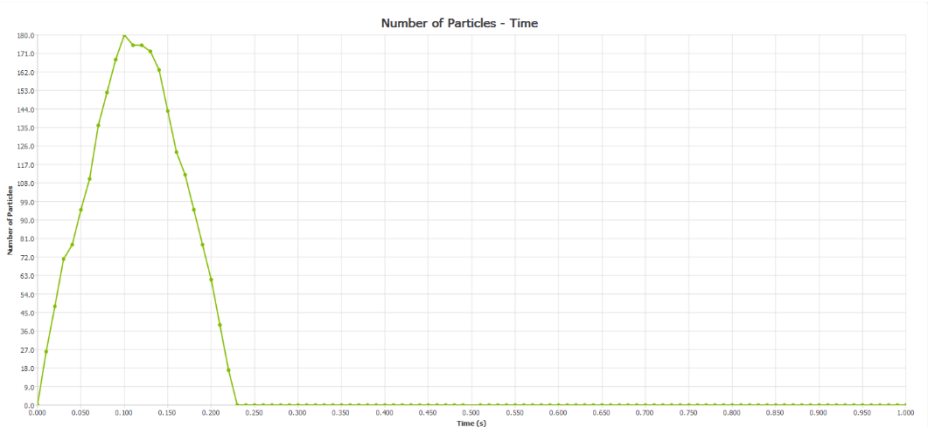

Figure 22 V Tube, Second Modal Frequency

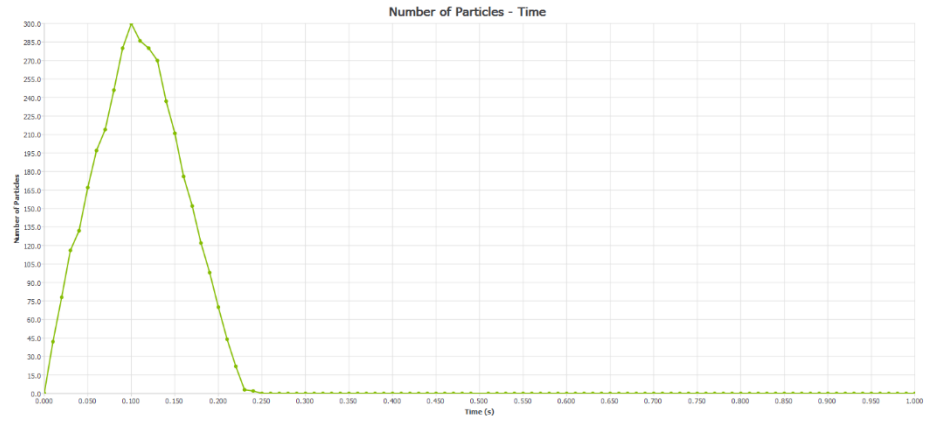

Figure 23 V Tube, Third Modal Frequency

All three modes are incredibly similar. All particles leave the tube within 0.25 seconds. Like the straight tube, it has an incredibly simple geometry which does not hinder the flow of powder out of the tube which explains this high flow rate of particles.

5.2.1.5. Dynamic Mode Conclusion

The findings do not accurately model the flow of excess powder, and very few conclusions can be drawn from these results apart from the behaviour of a very small number of particles. The key result obtained is the specific modal frequencies which allow a small number of particles to escape the tube and therefore can be investigated further to see the flowability of a considerably larger sample of particles. The table of modes that will be investigated further is shown in the table below.

	Modal Frequency		
	1st	2nd	3rd
Straight Tube			
S Tube			
U Tube			
V Tube			

Table 7 Summarising the successful dynamic factory results

5.2.2. Static Factory at the Boundary Layer

To build up a more detailed picture of the flow of the powder a static factory was used as described in section 4.3.3. This is not using a full number of particles, but the simulation time did increase dramatically.

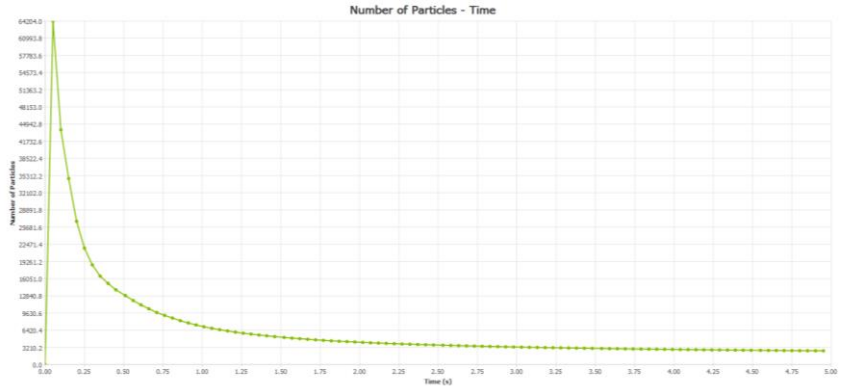

Figure 24 S Tube, Static Factory First Mode

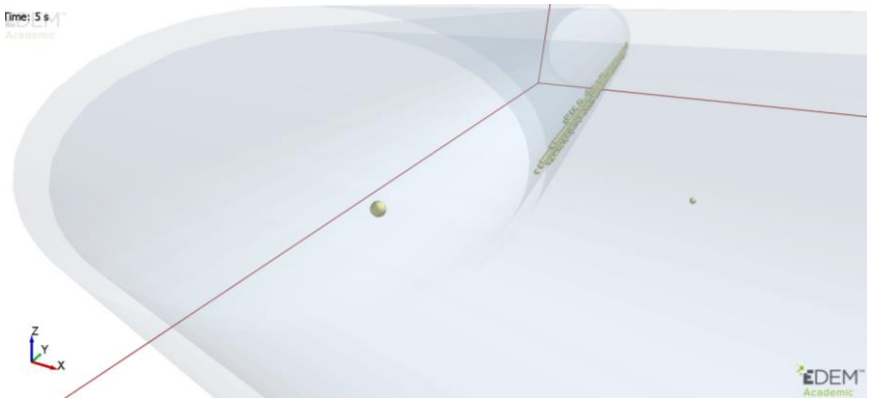

Figure 25 S Tube, Static Factory First Mode at 5 seconds

The results obtained are very similar to that obtained from the dynamic factory. There was initially a large flow of particles at the beginning, but this then was slowed down. Although the results were good and match what was previously expected, due the collisions at the boundary layer being a major approximation to the overall removal of powder focusing on the internal static factory. Due to simulations taking a long time to run, it was decided to move on to internal static factories which is slightly more computationally heavy but gave a more accurate representation of the flow a larger sample of powder.

5.2.3. Internal Static Factory

Due to the length of time and memory taken to run a simulation the first 0.2 seconds were originally simulated. The time of these simulations were than extended depending on the conclusions drawn from the initial 0.2 seconds.

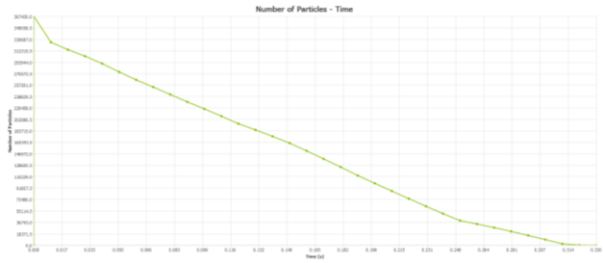

Figure 26 Straight Tube First Mode x direction

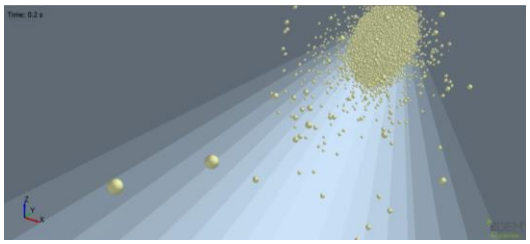

Figure 27 Straight Tube First Mode x direction showing the particles left at 0.2 seconds

The particle flow out of the straight tube is at a very consistent and linear for the first modal frequency acting in the x direction. The majority of particles had left the tube by 0.2 seconds, the few that remained were located at the centre of the tube in a cluster. From this cluster, the particles collided with each other and the edge of the tube and slowly worked their way out.

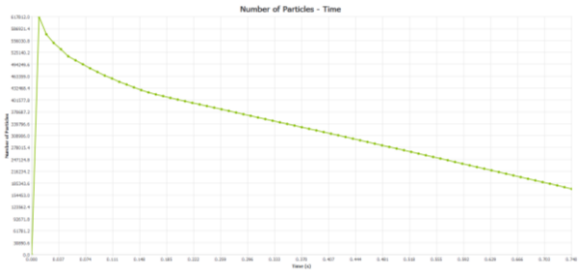

Figure 28 Straight Tube First Mode z direction

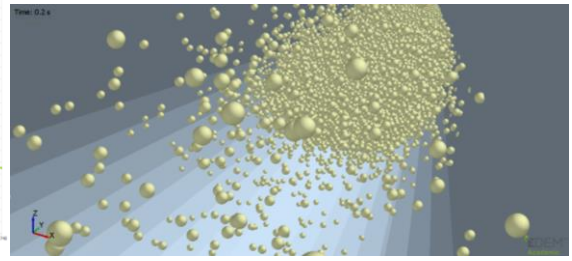

Figure 29 Straight Tube First Mode z direction showing the particles left at 0.2 seconds

The particle flow for the first mode of the straight tube is incredibly similar in the x and z directions, with the expectation that it takes a lot longer for particles for vibrations in the z direction. This was due to gravity acting in the same direction as the oscillations of the tube, meaning that major collisions were only happening in one direction rather than two as with the previous example.

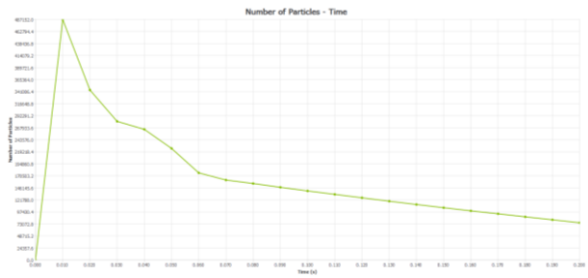

Figure 30 S Tube Second Mode

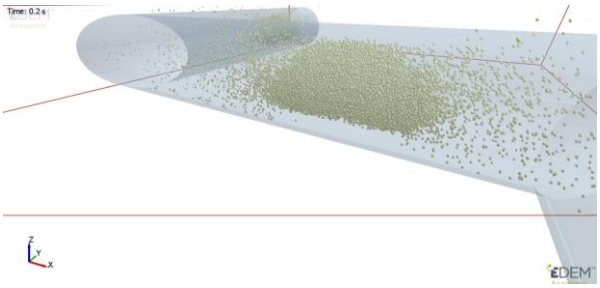

Figure 31 S Tube Second Mode showing the particles left at 0.2 seconds

For the S tube second mode, there are three regions of particles, all in the middle of the three separate tubular sections. Initially, there was a large flow of powder out of the tube, this then slowed down to a very linear rate of flow from the tube.

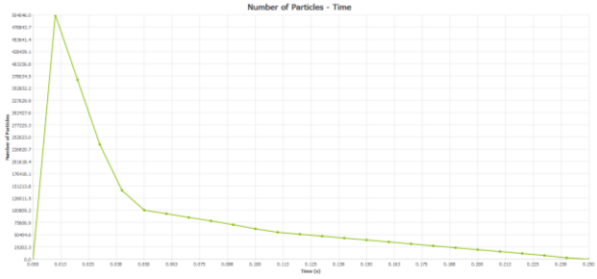

Figure 32 U Tube Second mode

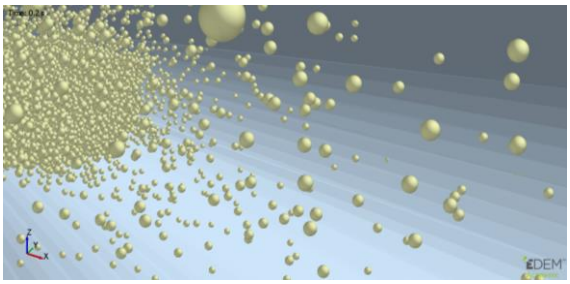

Figure 33U Tube Second Mode, showing the particles left at 0.2 seconds

For the U tube second mode, the vast majority of the particles left within the first 0.05 seconds, this was from the two ends of the U tube. It was more difficult to remove the powder from the central section of the tube, so a cluster formed.

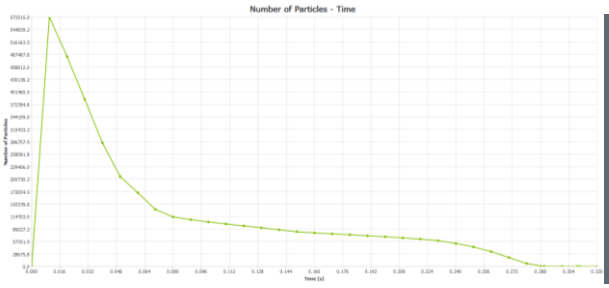

Figure 34 V Tube First Mode

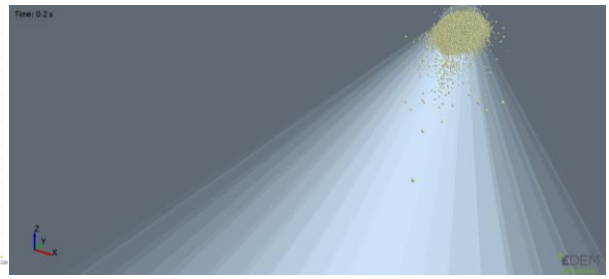

Figure 35 V tube first mode, showing the particles left at 0.2 seconds

Testing the first V tube mode, all the particles left the tube by 0.3 seconds; the majority left via the tube parallel to the y axis.

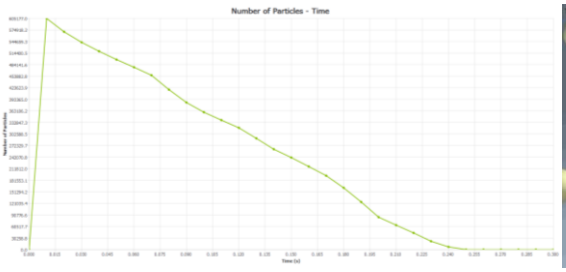

Figure 36 V Tube Second Mode

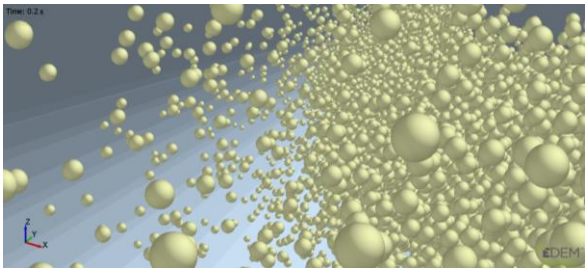

Figure 37V Tube Second Mode, showing the particles at 0.2 seconds

The second V tube mode showed a very linear flow out of the tube, the flow of particles left almost equally from both sections of the tube.

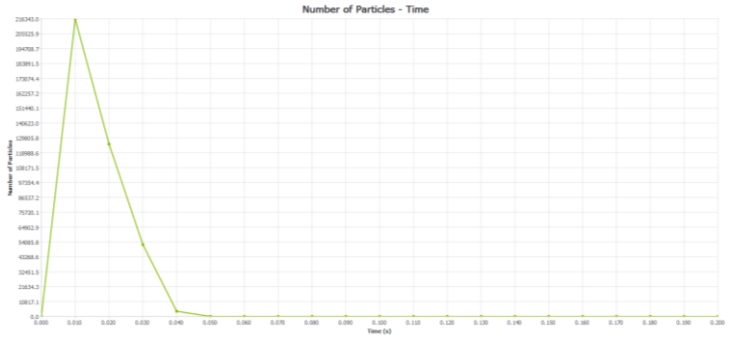

Figure 38 V Tube Third Mode

The third mode V tube vibrations were modelled by translations in the x and y direction, because of this the particles left extremely quickly from either end of the tube. All the particles left by 0.06 seconds, so for the sake of comparison, an image of the flow has not been included.

Simulation	Initial Flow Rate (Particles per Second)	Stabilised Flow Rate (Particles per Second)	Percentage Difference (x)
Straight Tube 1st Mode x	-1837140	-1217125	-33.7
Straight Tube 1st mode z	-4633600	-417441	-91.0
S Tube 2nd Mode	-14117300	-608925	-95.7
U tube 2nd Mode	-13231200	-537647	-95.9
V Tube 1st Mode	-5416500	-430138	-92.1
V Tube 2nd Mode	-3328500	-2445933	-26.5
V Tube 2nd Mode	-9086500	-4921750	-45.8

Table 8 showing the initial and stabilised gradients for the internal static factories

The table above shows the different initial flow rate of particles out of the tube as well as the stabilised flow rates. The reason why the initial flow rate was so large is that as the tubes were constantly full, the powder at the end of the tubes simply fell out and was not hindered by the shape of the tube or the other particles, this explains why there is such a large difference between the initial and stabilised flow out of the tube.

The shape of the tube had a great effect on the flow out of the tube the straight tubes took the shortest time to show a linear flow rate out of the tube. Conversely, the tubes that had multiple bends such as the S and U tubes took longer to stabilise to a linear flow rate.

6. Discussion and conclusions

This report has built and developed a successful way of modelling the flow of excess powder from additive layer manufacturing using DEM. The inherent complications of DEM, such as the length of the simulation time has been reduced by the procedure this report has developed. The use of modal analysis was used to reduce the number of frequencies that needed to be simulated and maximise the displacement of the oscillations. This saved time and lead to more efficient simulations. The use of dynamic factories was key as they reduced the simulation time significantly and gauged which modal shapes were effective at removing the powder. The

results gained here determined which modal shapes were taken forward and investigated further and which ones were inefficient and could be ignored. The detailed simulations involving the internal static factory gave detailed solutions of the flow of powder at specific frequencies. These simulations took a long time to run; initially, it was difficult to predict how long each simulation would take, so a very small run time was set, which could be extended if it needed to be.

The findings and processes from this report can be taken further to more complex parts and ultimately lead to increase the efficiency of the powder removal process if ALM would ever become a mass production manufacturing technique. The models of flow rate from the tubes can be taken further by validating the results. As discussed in the literature review, currently this is done experimentally.

7. Project management, consideration of sustainability and health and safety

7.1. Project Management

Throughout this project, the plan changed slightly. EDEM tutorials took longer than expected and more time was used getting to a point where usable results were calculated. It was decided not to obtain experimental data as a form of validation, as it would be expensive to produce the components and that time would be better spent focusing in more detail on the discrete element method. The downside of this is that the models produced will not be validated.

Following the Gantt chart ensured efficient project planning, the key milestones of this project were; finishing the modal analysis, modelling using the static factories and finishing the detailed DEM simulations.

Task Name	Duration	Start	Finish
Continue Background Reading and Reasearch	24 days	Thu 18/01/18	Tue 20/02/18
Create CAD Models to be Tested	2 days	Thu 18/01/18	Fri 19/01/18
Finite Element Analasis	11 days	Wed 24/01/18	Wed 07/02/18
DEM Tutorials	24 days	Thu 08/02/18	Tue 13/03/18
DEM Dynamic Factories	9 days	Wed 14/03/18	Mon 26/03/18
DEM Static Factories and Detailed Simulations	18 days	Tue 27/03/18	Thu 19/04/18
Start Writing about Background Research and Theory	28 days	Mon 12/03/18	Wed 18/04/18
Produce Final Report	10 days	Fri 20/04/18	Thu 03/05/18
Proof Read and Submit	3 days	Fri 04/05/18	Tue 08/05/18

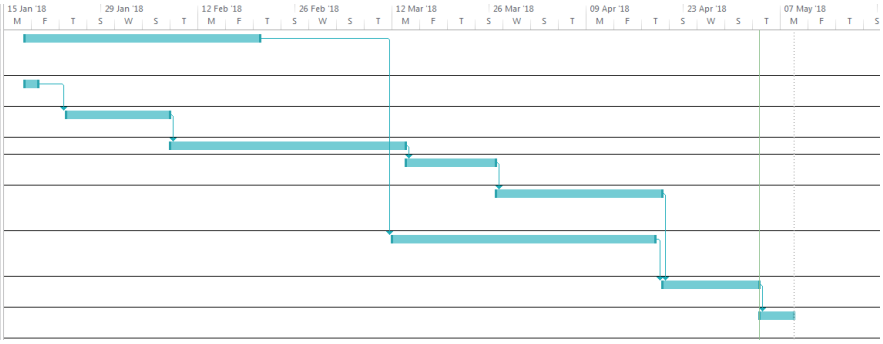

Figure 39 Showing Gantt chart

7.2. Sustainability

In recent years the importance of being sustainable is being pushed by governments, consumers as well as businesses. A major advantage of ALM is that it dramatically reduces waste material compared to a milling machine or other forms of subtractive manufacture. Less energy is also

required than traditional casting or forging techniques which require high temperatures and pressures. This energy is normally sourced from unsustainable methods of power generation such as coal or gas.

7.3. Health and Safety

As this was a simulation-based project health and safety was not considered as an issue as all the work was carried out on a computer there were no clear and obvious risks present to the operator.

8. References

[1] M. Akrami, "Manufacturing Methods ECM 3154," 2017. [Online]. Available: http://vle.exeter.ac.uk/mod/folder/view.php?id=653580. [Accessed 16 January 2018].

[2] D. a. R. Gault, "A comparison of rapid prototyping technologies," *International Journal of Machine Tools and Manufacture,* vol. 38, no. 10-11, pp. 1257-1287, 1998.

[3] Chegg, "Finite Element Analysis," Chegg Study, 2018. [Online]. Available: http://www.chegg.com/homework-help/definitions/finite-element-analysis-5. [Accessed 29 January 2018].

[4] G. Strang, "What is FEA?," SimScale, 2007. [Online]. Available: https://www.simscale.com/docs/content/simwiki/fea/whatisfea.html. [Accessed 29 January 2018].

[5] Jenike and Johanson, "Discrete Element Modeling," Jenike and Johanson, [Online]. Available: http://jenike.com/discrete-element-modeling/. [Accessed 10 Febuary 2018].

[6] O. Skrinjar, "On discrete element modelling of compaction of powders with size ratio," *Computational Computer Science,* vol. 31, no. 1-2, pp. 131-146, 2004.

[7] L. M. C, "Discrete element modeling of metallic powder sintering," *Scripta Materialia,* vol. 55, no. 5, pp. 425-428, 2006.

[8] R. K. W, "Process modeling in the pharmaceutical industry using the discrete element method," *Journal of Pharmaceutical Science ,* vol. 98, no. 2, pp. 442-470, 2009.

[9] L. H, "Using the discrete element method to analyze the breakage rate in a centrifugal/vibration mill," *Powder Technology,* vol. 198, no. 3, pp. 364-372, 2009.

[10] "Natural Frequency," Chegg Study, 2018. [Online]. Available: http://www.chegg.com/homework-help/definitions/natural-frequency-5. [Accessed 20 Febuary 2018].

[11] Bocko, Pavol Lengvarsky and Jozef, "Theoretical Basis of Modal Analysis," 2013.

[12] C. Rusu, "What is FEA modal analysis?," FEA for all, November 2016. [Online]. Available: https://feaforall.com/what-modal-analysis-fea-basics/. [Accessed 20 Febuary 2018].

[13] C. W. Smith, "Ansys ECM3173," 2017. [Online]. Available: http://vle.exeter.ac.uk/course/view.php?id=6375. [Accessed 22 February 2018].

[14] Nafems, "The Importance of Mesh Convergence," [Online]. Available: https://www.nafems.org/join/resources/knowledgebase/001/. [Accessed 14 March 2018].

[15] Comsol, "What Is Finite Element Mesh Refinement," Comsol, [Online]. Available: https://www.comsol.com/multiphysics/mesh-refinement. [Accessed 14 March 2018].

[16] H. Attar, "Effect of Powder Particle Shape on the Properties of In Situ Ti–TiB Composite Materials Produced by Selective Laser Melting," *Journal of Material Science Technology* , vol. 31, no. 10, pp. 1001-1005, 2015.

[17] Renishaw, "Metal Powders for AM," Reinshaw, [Online]. Available: http://www.renishaw.com/en/metal-powders-for-am--31457. [Accessed 28 January 2018].

[18] B. W. A Wank, "High Energy Ball Milling- A Promising Route for Production of Tailored Thermal Spray Consumabales," *Conference of Modern Wear and Corrosion Coatings,* pp. 1-10, 2003.

[19] A. Simchi, "Direct laser sintering of metal powders: Mechanism, kinetics and microstructural features," *Materials Science and Engineering: A,* vol. 428, no. 1-2, pp. 148-158, 2006.

[20] B. Peng, "Discrete Element Method (DEM) Contact Models Applied to Pavement Simulation," *Civil Engineering: Virginia Polytechnic Institute and State University,* vol. 1, no. 1, pp. 1-68, 2014.

[21] N. J. C. J. F. &. O. J. Y. Brown, "A bond model for DEM simulation of cementitious materials and," Springer-Verlag Berlin Heidelberg, Queens University Belfast, 2014.

[22] EDEM, "DEM Solutions Releases EDEM 2.4 for Research and Teaching," EDEM, 16 September 2011. [Online]. Available: https://www.edemsimulation.com/news/dem-solutions-releases-edem-24-for-research-and-teaching/.

[23] T. S. Y. a. S.-U. C. Junghwoon Lee, “The Effect of Particle Size on Thermal Conduction in Granular Mixtures,” *MDPI Materials,* vol. 8, no. 7, pp. 3975-3991, 2015.

[24] EDEM, “EDEM Simulation Linear Cohesion,” EDEM, March 2017. [Online]. Available: https://www.edemsimulation.com/content/uploads/2017/03/LinearCohesionV2_guide.pdf . [Accessed 16 March 2018].

[25] M. P. d. S. B. Helio A. Navarro, “LINEAR AND NONLINEAR HERTIZIAN CONTACT MODELS FOR,” *International Congress of Mechanical Engineering,* vol. 1, no. 1, pp. 159-170, 2013.

[26] R. Kievitsbosch, “Influence of dry cohesion on the micro- and macro-mechanical properties of dense polydisperse powders & grains,” *EPJ Web of Conferences,* p. 140, 2017.

[27] EDEM, “Overview of EDEM,” EDEM, [Online]. Available: https://www.edemsimulation.com/lessons/overview-of-edem/. [Accessed 20 March 2018].

[28] EDEM, “Creating materials,” EDEM, [Online]. Available: https://www.edemsimulation.com/topic/creating-materials-2/. [Accessed 20th March 2018].

[29] A. H. a. K. A. Ismail, “Coefficient of restitution of sports balls: A normal,” *IOP Conference Series: Materials Science and Engineering,* vol. 36, no. 1, pp. 1-8, 2012.

[30] Hyper Physics, “Static Friction,” Hyper Physics, [Online]. Available: http://hyperphysics.phy-astr.gsu.edu/hbase/frict2.html. [Accessed 13 March 2018].

[31] The Engineering ToolBox, “Rolling friction and rolling resistance,” The Engineering ToolBox, [Online]. Available: https://www.engineeringtoolbox.com/rolling-friction-resistance-d_1303.html. [Accessed 13 March 2018].

[32] EDEM, “Creating multi-sphere particles,” EDEM, [Online]. Available: https://www.edemsimulation.com/topic/creating-multi-sphere-particles-2/. [Accessed 20 March 2018].

[33] EDEM, [Online]. Available: https://www.edemsimulation.com/topic/creating-built-geometry-parts/. [Accessed 22 March 2018].

[34] EDEM, “Creating equipment using CAD files,” EDEM. [Online]. [Accessed 22 March 2018].

[35] EDEM, “Static and dynamic factories,” EDEM, [Online]. Available: https://www.edemsimulation.com/topic/static-dynamic-factories/. [Accessed 22 March 2018].

[36] EDEM, “Factory parameters,” EDEM, [Online]. Available: https://www.edemsimulation.com/topic/factory-parameters-2/. [Accessed 22 March 2018].

[37] EDEM, “Assigning geometry kinematics,” EDEM, [Online]. Available: https://www.edemsimulation.com/topic/assigning-geometry-kinematics/. [Accessed 22 March 2018].

[38] EDEM, “EDEM Creator: environment section,” EDEM, [Online]. Available: https://www.edemsimulation.com/lessons/edem-creator-environment-section/. [Accessed 22 March 2018].

[39] EDEM, “Setting Simulator options,” [Online]. Available: https://www.edemsimulation.com/topic/setting-simulator-options-2/. [Accessed 22 March 2018].

[40] Areospace Specification Materials, “Titanium Ti-6Al-4V (Grade 5),” Areospace Specification Materials, [Online]. Available: http://asm.matweb.com/search/SpecificMaterial.asp?bassnum=mtp641. [Accessed 10 March 2018].